Title

Single-Site Zeolite-Anchored Organoiridium Carbonyl Complexes: Characterization of Structure and Reactivity by Spectroscopy and Computational Chemistry

Journal

Chemistry - A European Journal, 21(33)

ISSN

0947-6539

Authors

Martinez-Macias, Claudia
Chen, Mingyang
Dixon, David A
et al.

Publication Date

2015-08-10

DOI

10.1002/chem.201501277

Peer reviewed

Single-Site Zeolite-Anchored Organoiridium Carbonyl Complexes: Characterization of Structure and Reactivity by Spectroscopy and Computational Chemistry

Claudia Martinez-Macias[a], Mingyang Chen[b,c], David A. Dixon[b], and Bruce C. Gates*[a]

[a] Prof. B. C. Gates and C. Martinez-Macias
Department of Chemical Engineering and Materials Science
University of California, Davis
One Shields Avenue, Davis, California, 95616, USA
E-mail: bcgates@ucdavis.edu

[b] Prof. D. A. Dixon and Dr. M. Chen
Department of Chemistry
University of Alabama
Tuscaloosa, Alabama, 35487, USA

[c] Dr. M. Chen
National Center for Computational Sciences
Oak Ridge National Laboratory
Oak Ridge, Tennessee, 37831, USA

Supporting information for this article is given via a link at the end of the document.

Abstract: A family of HY zeolite-supported cationic organoiridium carbonyl complexes was formed by reaction of $Ir(CO)_2(acac)$ (acac = acetylacetonate) to form supported $Ir(CO)_2$ complexes, which were treated at 298 K and 1 atm with flowing gas-phase reactants, including C_2H_4, H_2, ^{12}CO, ^{13}CO, and D_2O. Mass spectrometry was used to identify effluent gases, and infrared and X-ray absorption spectroscopies were used to characterize the supported species, with the results bolstered by DFT calculations. Because the support is crystalline and presents a nearly uniform array of bonding sites for the iridium species, these were characterized by a high degree of uniformity, which allowed a precise determination of the species involved in the replacement, for example, of one CO ligand of each $Ir(CO)_2$ complex with ethylene. The supported species include the following: $Ir(CO)_2$, $Ir(CO)(C_2H_4)_2$, $Ir(CO)(C_2H_4)$, $Ir(CO)(C_2H_5)$, and (tentatively) Ir(CO)(H). The data determine a reaction network involving all of these species.

Introduction

Some of the best-defined supported catalysts consist of single-metal-atom complexes bonded to supports. Such catalysts find industrial applications for processes including methanol carbonylation[1] and alkene polymerization[2] and are drawing increased attention because they offer opportunities for new properties combined with the most efficient use of the metals.[3] When such catalysts are synthesized to be highly uniform, their chemistry can be tuned precisely with methods that essentially match those of solution organometallic chemistry. The degree of uniformity of a supported catalyst is maximized when the support, which is a ligand for the metal, is highly uniform—hence crystalline—providing well-defined bonding sites. Thus, zeolites provide platforms for the synthesis of uniform supported metal complexes that can be characterized incisively, as has been demonstrated for metals including ruthenium,[4] rhodium,[5] iridium,[6] and gold.[7]

Essentially molecular species on crystalline supports provide excellent opportunities for fundamental understanding of site-isolated catalysts, and our goal was to prepare a family of such species[8] with systematically varied ligands chosen to tune the reactivity and facilitate the structural characterization. We report results characterizing zeolite Y-supported iridium complexes incorporating CO ligands, which are ideal because the CO stretching frequencies are readily measured by infrared (IR) spectroscopy and provide insight into the electronic properties of the metal atom and its environment. We report data characterizing a family of iridium carbonyls formed by treatment with flowing gases that react with the metal, resulting in ligand exchange. Analysis of the effluent gases by mass spectrometry and investigation of the supported species by IR and extended X-ray absorption fine structure (EXAFS) spectroscopies complemented with X-ray absorption near edge structure (XANES) and calculations at the level of density functional theory (DFT) enabled the determination of the structures of the supported species and the reaction pathways by which they are converted. The supported iridium carbonyls are some of the best-characterized supported metal species.

Results

IR spectra show that $Ir(CO)_2(acac)$ reacted with the zeolite to form zeolite-supported iridium *gem*-dicarbonyls, $Ir(CO)_2$, and these have been reported to undergo reactions whereby one carbonyl ligand is replaced by ethylene.[9] This synthesis afforded us the opportunity to characterize a family of zeolite-supported iridium complexes formed by exchange of the reactive ethylene ligand, with the remaining CO ligand providing valuable information about the structure. Thus, we have determined a reaction network involving the replacement of various ligands on the iridium, as summarized below. The ligand replacement reactions were carried out with the solid samples in contact with gas-phase reactants, some of them being isotopically labeled (^{13}CO and D_2O).

Structural characterization of initially prepared zeolite-supported iridium complexes

IR spectra show that as $Ir(CO)_2(acac)$ reacted with surface OH groups of dealuminated zeolite HY the intensity of the 3630-cm^{-1}

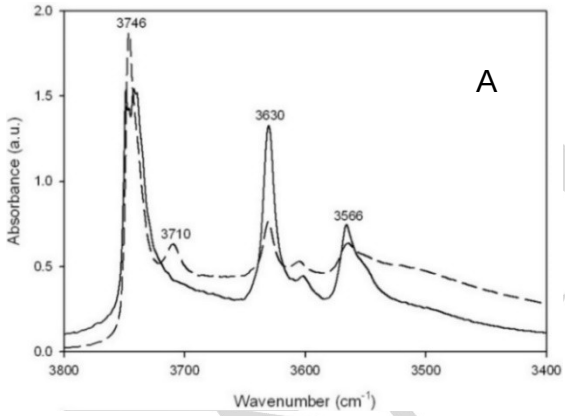

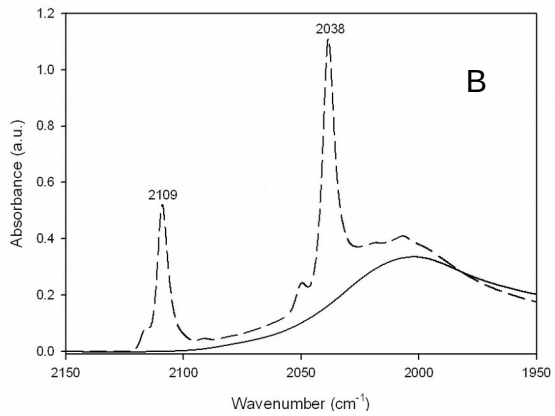

Figure 1. IR spectra characterizing the bare zeolite (solid line) and the zeolite after reaction with $Ir(CO)_2(acac)$ (dashed line) in (A) the OH region and (B) the carbonyl region.

band assigned to isolated OH groups bonded at Al sites in the zeolite supercages decreased by approximately 46% (Figure 1A).[10,11] These results demonstrate that the supported cationic iridium complexes were bonded where there had been acidic sites in the zeolite supercages, as expected, and reacted with only a fraction of these sites. The acac ligands were correspondingly largely converted to Hacac, as indicated by the IR spectra (SI, Figure S1).[12]

The IR spectra characterizing the resultant supported iridium complex (Figure 1B) indicate that it retained the carbonyl ligands, as shown by the ν_{CO} bands at 2109 and 2038 cm^{-1}, which are assigned to mononuclear iridium *gem*-dicarbonyls.[13,14] The sharpness of these ν_{CO} bands (full width at half-maximum ~5 cm^{-1}) indicates highly uniform supported iridium species.[15,16]

In agreement with the IR data, EXAFS spectra recorded at the Ir L_{III} edge (Table 1) confirm that the iridium was bonded on average (and within error) to two CO ligands. The EXAFS data

Table 1. Summary of EXAFS fit parameters[a] and vibrational frequencies characterizing zeolite-supported iridium complexes at 298 K and 1 bar.

	EXAFS results						
Sample/treatment conditions	Absorber-backscatterer pair	*N*	*R* (Å)	$10^3 \times \Delta\sigma^2$ (Å^2)	ΔE_0 (eV)	Frequencies of bands in ν_{CO} region of IR spectra (cm^{-1})	Supported iridium species inferred from data
$Ir(CO)_2$ in helium	$Ir–O_{zeolite}$	2.0	2.06	2.7	-3.4	2109, 2038	$Ir(CO)_2$
	$Ir–C_{CO}$	2.0	1.97	6.3	3.6		
	$Ir–O_{CO}$	2.0	2.94	8.3	-7.7		
	$Ir–Al_{zeolite}$	0.9	2.73	3.1	2.4		
Sample formed from $Ir(CO)_2$ in C_2H_4	$Ir–O_{zeolite}$ and $Ir–C_{C2H4}$	4.5	2.01	7.5	-2.2	2087	$Ir(CO)(C_2H_4)_2$
	$Ir–C_{CO}$	1.0	1.83	3.0	0.1		
	$Ir–O_{CO}$	1.0	2.95	3.4	-6.4	2055	$Ir(CO)(C_2H_4)$
	$Ir–Al_{zeolite}$	1.0	2.77	3.7	1.0		
Preceding sample after 70 min in H_2	$Ir–O_{zeolite}$ and $Ir–C_{C2H5}$	2.6	2.07	3.9	-7.2	2075	$Ir(CO)(C_2H_5)$
	$Ir–C_{CO}$	1.0	1.99	2.1	-3.5		
	$Ir–O_{CO}$	1.0	2.94	1.2	-3.5		
	$Ir–Al_{zeolite}$	1.0	2.78	1.1	-0.2		
Preceding sample after an additional 50 min in H_2	$Ir–O_{zeolite}$	2.0	2.05	1.0	-7.8	2068	$Ir(CO)(H)_x$
	$Ir–C_{CO}$	1.0	1.96	0.8	4.5		
	$Ir–O_{CO}$	1.0	2.94	2.0	-1.8		
	$Ir–Al_{zeolite}$	1.0	2.76	2.8	4.3		

[a] Notation: *N*, coordination number; *R*, distance between absorber and backscatterer atoms; $\Delta\sigma^2$, disorder term (Debye-Waller factor); ΔE_0, inner potential correction. Error bounds characterizing the structure parameters obtained by EXAFS spectroscopy are estimated to be as follows: *N*, ± 20%; *R*, ± 0.02 Å; $\Delta\sigma^2$, ± 20%; and inner potential correction ΔE_0, ± 20%. However, the errors in the parameters characterizing the Ir–Al contribution are greater than those characterizing the other contributions, and the data are not sufficient for good estimates of the uncertainties in these values.

further demonstrate that each Ir atom was bonded, on average, to two support oxygen atoms; thus, the support acted as a bidentate ligand. This result is as expected on the basis of results obtained with various metal oxide and zeolite supports reacting with the same precursor.[17]

Reactions of supported iridium dicarbonyl complexes with C_2H_4 and with H_2

When the zeolite-supported iridium dicarbonyl was exposed to flowing ethylene at 298 K, changes in the IR and EXAFS spectra were observed. The initial ν_{CO} bands at 2109 and 2038 cm^{-1}, corresponding to the ν_s and ν_{as} vibrations of $Ir(CO)_2$, disappeared within 4 min, with the simultaneous growing in of new bands at 2087 and 2054 cm^{-1} (Figure 2), assigned to $Ir(CO)(C_2H_4)_2$ and $Ir(CO)(C_2H_4)$, respectively, consistent with an earlier report.[9] Furthermore, the EXAFS data (Table 1) show that the $Ir–C_{CO}$ and $Ir–O_{CO}$ coordination numbers decreased from nearly 2 to nearly 1, indicating the removal of one of the two initially present CO ligands of the iridium complex. At the same time, the coordination number of the EXAFS contribution characterizing the sum of $Ir–O_{zeolite}$ + $Ir–C_{ethylene}$ contributions (the data were not sufficient to resolve these) increased from nearly 2 to nearly 4.5 (Table 1). These data indicate replacement of carbonyl ligands by ethylene, and the non-integer value of the combined $Ir–O_{zeolite}$ + $Ir–C_{ethylene}$ contribution indicates a mixture of species, consistent with the IR spectra pointing to both $Ir(CO)(C_2H_4)$ and $Ir(CO)(C_2H_4)_2$ species (Figure 2).

The shoulder in the IR spectrum at 2047 cm^{-1} (Figure 2), present only for the sample formed from $Ir(CO)_2$/HY zeolite in ethylene, matches that assigned to $Ir(CO)(C_2H_4)_2$ species bonded to Al_2O_3.[18] It has been reported[19] that dealuminated zeolites, such as the HY zeolite used in the present work,

contain small regions of amorphous material resulting from the dealumination process, and, when the precursor metal complex reacts with the support, it is expected to bond to these regions as well as the crystalline regions. Thus, we infer that the 2047-cm^{-1} shoulder gives evidence of iridium bonded to the surface within the small amorphous regions of the support. This band disappeared when the flow of ethylene over the sample stopped, indicating that the $Ir(CO)(C_2H_4)_2$ complexes bonded to the amorphous regions of the support are stable in the presence of ethylene at 298 K but not in its absence.

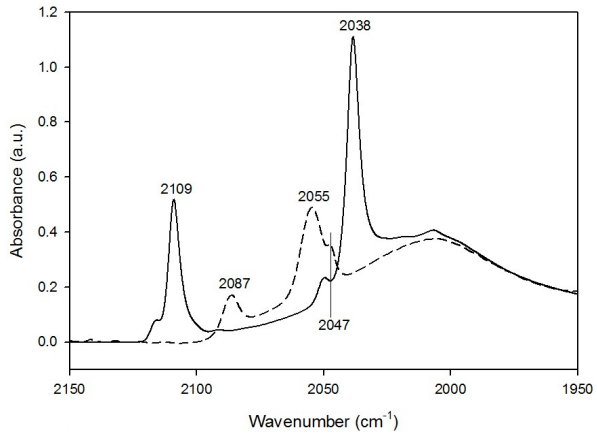

Figure 2. IR spectra of $Ir(CO)_2$/HY zeolite in flowing helium (solid line) and in flowing ethylene (dashed line).

The family of samples was expanded by further treatment, as follows. After contacting of the sample incorporating $Ir(CO)_2$ complexes (~30 mg) with ethylene, it was brought in contact with H_2 at 298 K and 1 bar flowing at a rate of 50 mL/min, leading to the following changes. The 2087-cm^{-1} band, assigned to supported $Ir(CO)(C_2H_4)_2$ species,[9] started decreasing in intensity, disappearing after 45 min (Figure 3A). After the disappearance of this band (Figure 3A), the band at 2055 cm^{-1}, assigned to supported $Ir(CO)(C_2H_4)$ species,[9] started to decrease in intensity, as a new band appeared at 2075 cm^{-1} (Figure 3A), reaching a maximum in intensity after 70 min of contact with H_2. Because

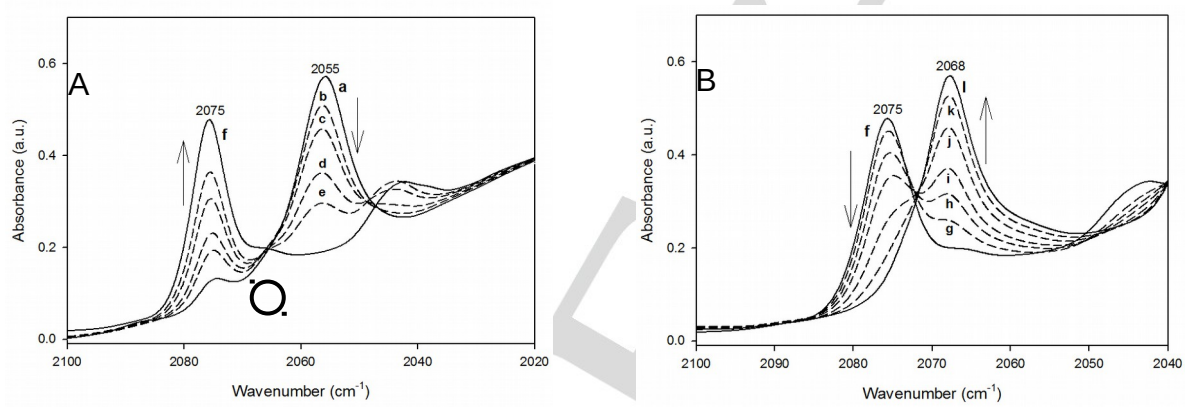

Figure 3. IR spectra of sample initially in the form of $Ir(CO)_2$/HY zeolite during treatment in flowing H_2 for the following times (min) all following the disappearance of the 2087 cm^{-1} band assigned to the $Ir(CO)(C_2H_4)_2$ complexes: (a) 45, (b) 55, (c) 59, (d) 63, (e) 65, (f) 70, (g) 76, (h) 80, (i) 84, (j) 91, (k) 103, and (l) 124. (A) Decrease in intensity of the 2055-cm^{-1} band accompanied by the growing in of the 2075-cm^{-1} band. (B) The intensity of the 2075-cm^{-1} band reached a maximum and started decreasing along with the appearance of the 2068-cm^{-1} band.

the 2055 cm^{-1} band assigned to $Ir(CO)(C_2H_4)$ disappeared along with the appearance of the new band only when H_2 was present, we infer that the ethylene ligand was being hydrogenated. The isosbestic point encircled in Figure 3A shows that the hydrogenation was stoichiometrically simple. As the 2075-cm^{-1} band started to decrease in intensity, a new band appeared at 2068 cm^{-1} (Figure 3B). We postulate that the supported species at the two stages of hydrogenation were $Ir(CO)(C_2H_5)$ and $Ir(CO)(H)_x$, respectively, where x is undetermined; we return to this point below.

In a different treatment, the sample initially present as $Ir(CO)_2$ was brought in contact with ethylene followed by a purge with helium at 298 K and 1 bar to remove the gas-phase ethylene. After this treatment, the 2087-cm^{-1} band (assigned to $Ir(CO)(C_2H_4)_2$ complexes) had disappeared, indicating removal of one of the ethylene ligands, but the 2055-cm^{-1} band (assigned to $Ir(CO)(C_2H_4)$ complexes) remained (Figure S2). Then the sample was treated with flowing H_2, and the 2075-cm^{-1} band (assigned to $Ir(CO)(C_2H_5)$ complexes) appeared, indicating the partial hydrogenation of the remaining ethylene ligands, and this

step was followed by the disappearance of this band as a new IR band appeared at 2068 cm^{-1}. The disappearance of the ethylene ligands was accompanied by the appearance of gas-phase ethane (detected by mass spectrometry in the effluent gas, SI, Figure S2), which demonstrates that the ethyl ligands were being hydrogenated.

Because (a) there was hydrogenation occurring and (b) the hydrocarbon ligands had been removed by hydrogenation, we assign the band that emerged at 2068 cm^{-1} to the ν_{CO} band of $Ir(CO)(H)_X$ complexes. In the experiments in which the helium purging step was included, the changes took place more quickly than when the sample cell was not purged with helium before the start of H_2 flow (Figure S2-A and B). The IR spectra recorded during the treatment that included the purging step are characterized by an isosbestic point (Figure S2-A, encircled). All the results are consistent with the assignment of the 2068-cm^{-1} band that emerged after hydrogenation of all the hydrocarbon ligands to $Ir(CO)(H)_X$.

To summarize, ethylene bonded to the iridium carbonyl underwent partial hydrogenation to give $Ir(CO)(C_2H_5)$ species bonded to the zeolite—characterized by the 2075-cm^{-1} band—and this reacted until the hydrocarbon ligands had been fully hydrogenated, giving gas-phase ethane and supported species that we formulate as iridium carbonyl hydrides, represented as $Ir(CO)(H)_X$—identified with the 2068-cm^{-1} band.

DFT calculations were performed to test the assignments. The calculations were performed with two separate models of the zeolite, a simple $Al(OH)_4$ model of the acid site and a much larger model, Zeo(48-T), with 48 Si/Al atoms (frequencies in Table 2). The calculations for the Zeo(48-T) model used scaling factors for the C–O and Ir–H stretches. We used a scaling factor of 1.062 for the C–O stretches from the ratio CO_{expt}/CO_{calc} and a scaling factor of 1.017 for the Ir–H stretches from the $H_{2,expt}/H_{2,calc}$ ratio.[20] The predicted ν_{CO} frequencies with the two models are in good agreement with the experimental values (Table 2) and bracket them, with the small model predicting slightly lower values than experiment and the scaled values from Zeo(48-T) predicting values slightly higher than experiment.

Table 2. Summary of vibrational frequencies (cm^{-1}) of the C–O stretch for the ligands of Ir(CO)(L)/HY zeolite.

Ligands	ν(C–O stretch)		Ref(s)
	DFT[a]	Experiment[b]	
CO/CO	2026/2058 2095/2136	2038, 2109[c]	This work, 9
CO/H	2055/2090	2068[d]	This work
CO/H_2	2053/2090		This work
CO/C_2H_4	2022/2053	2054[e]	This work, 9
CO/C_2H_5	2043/2094	2075[f]	This work

[a] First value is based on the simple $Al(OH)_4$ model. The second value, after the slash, is the Zeo(48-T) value scaled by 1.062 for the CO_{expt}/CO_{calc} ratio. [b] At 298 K and 1 bar. [c] $Ir(CO)_2$ in helium. [d] $Ir(CO)(H)_X$ in H_2. [e] $Ir(CO)(C_2H_4)$ in helium. [f] $Ir(CO)(C_2H_5)$ in H_2.

DFT calculations were also done in an attempt to identify the $Ir(CO)(H)_X$ complexes—as Ir(CO)(H) and/or $Ir(CO)(H)_2$. However, because the predicted wavenumber differences are small and the bands are predicted to be of comparable intensities (I = 640 km/mol for Ir(CO)(H) and I = 691 km/mol for $Ir(CO)(H)_2$ with the Zeo(48-T) model), we were at this stage still not able to distinguish between the two.

Treatment of $Ir(CO)_2$/HY zeolite with ^{13}CO

To strengthen the basis for identification of species containing CO ligands, each of the experiments with ethylene and H_2 described in the preceding sections was performed equivalently with ^{13}CO used instead of ^{12}CO in the complexes. Thus, the sample initially incorporating $Ir(CO)_2$ complexes (~30 mg) was treated with a pulse of ^{13}CO (14 molecules of ^{13}CO per Ir atom) to form $Ir(^{13}CO)_2$ complexes followed by the aforementioned treatment with C_2H_4 and H_2, to form a family of iridium complexes incorporating ^{13}CO. Data are shown in SI (Figures S4–S7), and a summary of the observed bands is presented in Table 3. The data are all consistent with the aforementioned assignments.

Table 3. Summary of IR bands in the νCO region characterizing samples incorporating zeolite-supported iridium complexes with ^{12}CO and ^{13}CO ligands.

Species incorporating CO ligands	^{12}CO stretching frequencies, cm^{-1}	^{13}CO stretching frequencies, cm^{-1}	^{13}CO stretching frequencies predicted from ^{12}CO stretching frequencies, cm^{-1} [a]
$Ir(CO)_2$	2109, 2038	2058, 1990	2062, 1993
$Ir(CO)(C_2H_4)_2$	2087	2040	2041
$Ir(CO)(C_2H_4)$	2055	2005	2009
$Ir(CO)(C_2H_5)$	2075	2026	2029
$Ir(CO)(H)_x$	2068	2018	2022

[a] Calculated from values based on ^{12}CO stretching frequencies with the harmonic approximation with the values reported.[22]

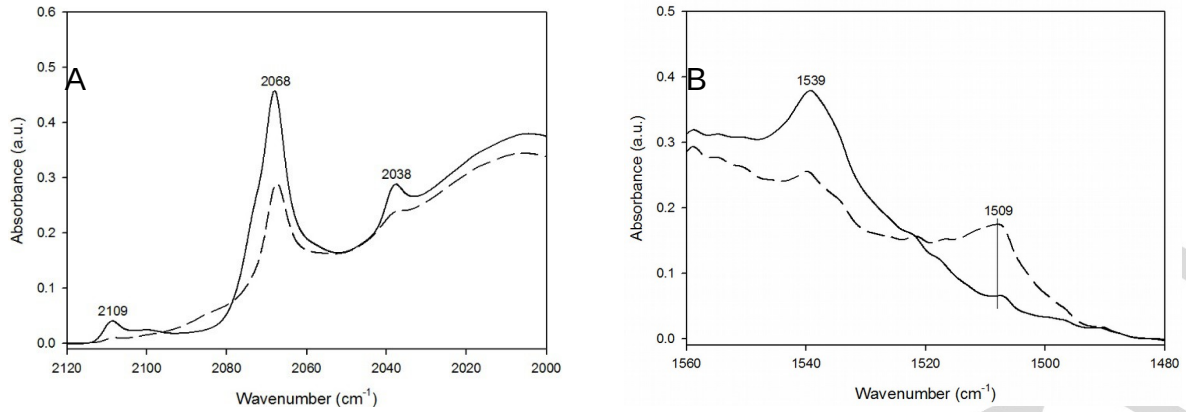

Figure 4. IR spectra of Ir(CO)(H)/HY zeolite (solid line) and after a D_2O pulse (dashed line) in flowing helium of (A) the carbonyl region and (B) the region between 1560 and 1480 cm^{-1}. Details related to these spectra are presented in the SI.

Reactions of $Ir(CO)(H)_X$/HY zeolite with D_2O and evidence of iridium hydride (deuteride) species

In an attempt to identify species incorporating hydride ligands, the sample initially incorporating the proposed $Ir(CO)(H)_X$ complexes after the aforementioned ethylene and H_2 treatments (and characterized by an IR band at 2068 cm^{-1} assigned to the C–O vibration) was exposed to D_2O. We anticipated that the D_2O would adsorb dissociatively on the acid sites of the zeolite and give D that by reverse spillover would react with the nearby iridium complexes.[21] In these experiments, the presumed $Ir(CO)(H)_X$/HY zeolite (~30 mg) was brought in contact with a pulse of helium (150 mL at 298 K and 1 bar) saturated with D_2O (Figure 4). After this treatment, the 2068-cm^{-1} band, corresponding to the C–O vibration of the $Ir(CO)(H)_X$ complexes, had decreased in intensity with the simultaneous growing in of a weak new band at 1509 cm^{-1}, which we suggest is evidence of Ir–D vibrations of iridium deuteride species. The band that corresponds to the C–O vibration of the Ir(CO)(D) complex, expected to appear at a lower wavenumber than the 2068-cm^{-1} band that corresponds to the C–O vibration of the Ir(CO)(H) complex, was not seen in the IR spectrum, because at approximately 2000 cm^{-1} there are strong, broad bands assigned to vibrations of the zeolite framework that evidently mask the C–O vibration of the Ir(CO)(D) complex.

To check the suggestion that the 1509-cm^{-1} band corresponds to an Ir–D vibration, the sample, after the D_2O treatment, was treated in flowing H_2 to determine whether the D would be replaced with H. The 1509-cm^{-1} band indeed decreased in intensity during the experiment (Figure S8), supporting our suggestion. The replacement of D by H was slow and not completed after 146 min of contact of the sample with flowing H_2, as expected.[23] No band indicative of an iridium hydride was evident in the resultant IR spectrum, consistent with the results mentioned above and the low intensities of such peaks—sometimes these are not even visible in the spectra of samples comparable to ours.[24]

Our samples also incorporated acac ligands bonded to the support with the ring vibrations bands at 1596, 1539, and 1366 cm^{-1} assigned to ν_{COring}, $\nu_{C–C–Cs}$, and δ_{CH}, respectively (Figure S1). Upon contact of the sample with D_2O, the bands assigned to $\nu_{C–C–Cs}$ and δ_{CH}, at 1539 and 1366 cm^{-1}, decreased in intensity, and, according to the calculated isotopic shift factor of 0.73 for C–H to C–D,[22] the deuterated bands were expected to appear at <1130 cm^{-1}, but these were not evident because of the strong absorption by the zeolite support in this region. Accordingly, we rule out the assignment of the 1509-cm^{-1} band to any deuterated acac vibration.

DFT calculations were carried out to provide a check of the suggested assignments. The results characterizing the Ir–H vibration of Ir(CO)(H) and $Ir(CO)(H)_2$ are presented in Table 4 for both zeolite models. The simple model gives lower values for the Ir–H stretching frequencies than the scaled Zeo(48-T) model, just as was found for the CO stretches. The predicted frequency of Ir(CO)(D) is 1591/1674 cm^{-1} (for the $Al(OH)_4$ and the Zeo(48-T) models respectively), in qualitative agreement with the observed value of 1509 cm^{-1}. Nonetheless, we recognize that the assignment of the IR band to Ir(CO)(D) is still less than definitive and that it could even represent Ir(D).

The Ir–H vibration characterizing the supported Ir(CO)(H) complexes is predicted to appear at about 2204/2360 cm^{-1} (according to the $Al(OH)_4$ and the Zeo(48-T) model respectively) and that characterizing the supported $Ir(CO)(H)_2$ complexes at 2348/2324 and 2480/2408 cm^{-1} (according to the $Al(OH)_4$ and the Zeo(48-T) model respectively, Table 4. We observed no bands in our IR spectra near these values, consistent with the predicted low infrared intensities of M–H vibrations.

We recognize that, in previous work,[25] samples similar to ours incorporating iridium complexes bonded to HY zeolite were characterized by an IR band at 2068 cm^{-1} (which we have attributed to a carbonyl band), and the authors suggested that it was evidence of an Ir–H vibration because they inferred that it

Table 4. Summary of the vibrational frequencies (cm^{-1}) determined by DFT calculations of the Ir–H stretch for the Ir(H)(L)/HY zeolite species

Ligand(s)	ν(Ir–H stretch) [b,c]	ν(Ir–D stretch) [b]
H[a] or D	2184/2336	1578/1657
H/H or D/D	2237/2471	1687/1753

	2293/2376	1654/1685
H/CO[a] or D/CO	2204/2360	1591/1674
H/H/CO or D/D/CO	2348/2480	1695/1759
	2324/2408	1677/1708

[a]doublet electronic state due to H. [b]First value is the simple $Al(OH)_4$ model. The second value, after the slash, is the Zeo(48-T) value scaled by 1.017 for the $H_{2,expt}$/ $H_{2,calc\ ratio}$. [c] Anharmonic corrections for the Ir-H stretches with the $Al(OH)_4$ model range from 75 to 110 cm^{-1}.

"shifted" to 1509 cm^{-1} after an isotopic exchange with D_2. However, the apparent shift does not match the frequencies calculated in the harmonic approximation,[22] and we suggest that it was indeed a carbonyl band (which might have arisen from trace CO impurities). We emphasize that our assignment of the 2068-cm^{-1} band is based on data from experiments done with ^{13}CO (Table 3) as well as our DFT calculations (Table 2).

To check for the possible presence of iridium hydride (or deuteride) complexes without CO ligands, that is, Ir(H) and $Ir(H)_2$ or Ir(D) and $Ir(D)_2$ complexes, additional DFT calculations were performed (Table 4). The predicted harmonic frequencies for the Ir–H vibration is 2184 cm^{-1} (for the simple $Al(OH)_4$ model) and 2336 cm^{-1} (for the Zeo(48-T) model) for the monohydride, Ir(H), and 2337 and 2293 cm^{-1} (for the simple $Al(OH)_4$ model) and 2471 and 2376 cm^{-1} (for the Zeo(48-T) model) for the dihydride, $Ir(H)_2$. Anharmonic corrections lower the Ir–H stretch by about 75 cm^{-1} and the Ir–H_2 stretches by about 110 cm^{-1}. We observed no such IR bands, but, again, the result might be explained by the low intensities expected for such IR bands. The predicted frequencies for the corresponding monodeuteride are 1578/1657 and for the dideuteride species are 1687/1753 and 1654/1685 cm^{-1} for the $Al(OH)_4$ and the Zeo(48-T) models, respectively. Correcting the Ir–D stretch with the inclusion of anharmonicity for the $Al(OH)_4$ model gives 1491 cm^{-1} (using a factor of $1/\sqrt{2}$). The 1509-cm^{-1} band observed in the IR spectrum of the deuterated sample (Figure 4B) is closer to our calculated values of 1578/1657 cm^{-1} (for the $Al(OH)_4$ and the Zeo(48-T) model, respectively) and could therefore be indicative of the monodeuteride species Ir(D). The presence of CO does not affect the Ir–H frequency for the monohydride by more than 20 cm^{-1}.

Calculations were also done for iridium hydride (and deuteride) samples incorporating hydrocarbon ligands (Table 4). The results show an Ir–H stretching vibration of 2101 cm^{-1} (which was not observed in the IR spectra) and also Ir–D vibrations characterizing $Ir(D)(C_2H_4)$ and $Ir(D)(C_2D_4)$ of 1544 and 1511 cm^{-1}, respectively. These are close to the experimental value of 1509 cm^{-1} found for our species that we infer to be an iridium deuteride complex, but we do not attribute the observed band to such species because the hydrocarbons had been removed from the sample.

Evidence of sample uniformity

The sharp ν_{CO} bands of the supported iridium carbonyls provide evidence of their structural uniformity, and the good fits of the EXAFS data complement the IR data. We emphasize that the EXAFS results represented in Table 1 all rest on a firm foundation both in terms of appropriate parameter values, overall good agreement between the data and the fit, and the successful fits to each individual absorber–backscatterer shell as indicated by the appropriateness of the fitting parameters.

But when we investigated the samples that incorporate hydride ligands (e.g., supported Ir(CO)(H) species—we stress that Ir–H contributions are not detectable by EXAFS spectroscopy) and considered several plausible structural models in the data fitting (in this example, not just Ir(CO)(H), but also $Ir(CO)(C_2H_4)(H)$, $Ir(CO)(C_2H_5)(H)$, $Ir(C_2H_4)_2(H)$, and $Ir(C_2H_4)(H)$), the results show that none of the plausible models incorporating hydrocarbons (Table S5) could be considered satisfactory by all of our aforementioned criteria. The fit for Ir(CO)(H) species is preferred because it is characterized by physically realistic values for all the contributions, a good overall fit, and *adequate* fits of the individual shells, but the evidence overall is less than fully satisfying—as would be expected if a mixture of species were present. Such reasoning contributes to our caution with regard to identification of each of the postulated hydride-containing (or deuteride-containing) species.

In summary, the data show that we have firm identifications of the supported iridium complexes that do not contain hydride or deuteride ligands, but that the identifications of the latter are less firm, and they might have been present in mixtures.

Reaction of supported iridium dicarbonyl complexes with H_2

Further experiments were done to check the reactivity of the supported $Ir(CO)_2$ complexes with H_2 directly at room temperature and atmospheric pressure. When the flow of H_2 over the sample started, a weak band appeared at 2173 cm^{-1} (Figure 5), but the carbonyl bands did not change measurably in intensity. This band has been assigned on the basis of reported data characterizing mononuclear zeolite-supported iridium species[14] to the symmetric C–O vibration of zeolite-supported $Ir^{2+}(CO)_2$, but we recognize, on the basis of the DFT-predicted frequencies (Table 4) and the foregoing results, that it might instead be attributed to the Ir–H vibration of Ir(H) species. The fact that the C–O vibrations of the initially present $Ir(CO)_2$ remained essentially unchanged suggests that the species characterized by the 2173-cm^{-1} band corresponds to a small fraction of the total iridium complexes. To confirm or rule out the assignment of the 2173-cm^{-1} band to a C–O vibration, we brought the initially present $Ir(CO)_2$ complexes in contact with a pulse of ^{13}CO (14 molecules of ^{13}CO per Ir atom) to form $Ir(^{13}CO)_2$ complexes, followed by the aforementioned treatment with H_2. The spectra recorded during the H_2 treatment show a very weak band at 2152 cm^{-1} (Figure S9) that has been assigned to zeolite- supported $Ir^{2+}(^{12}CO)(^{13}CO)$ complexes;[14] thus, we confirm the assignment of the 2173-cm^{-1} band to $Ir^{2+}(^{12}CO)_2$ complexes.

After the treatment leading to the appearance of the 2173-cm^{-1} band, the sample initially present as $Ir(^{12}CO)_2$, after

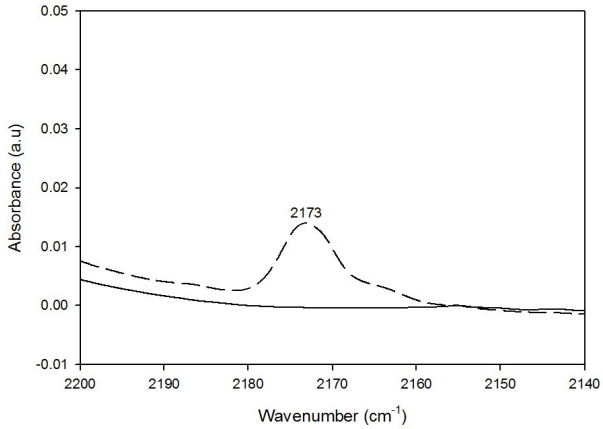

Figure 5. IR spectra of sample initially in form of $Ir(CO)_2$/HY zeolite in helium (solid line) and during H_2 treatment (dashed line).

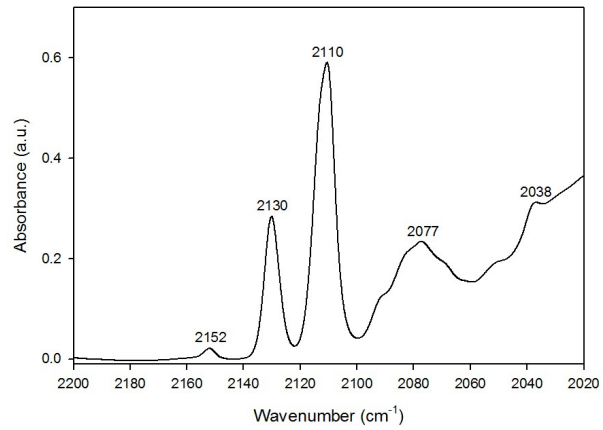

Figure 6. IR spectra of sample initially in form of $Ir(CO)_2$/HY zeolite after H_2 treatment followed by a CO pulse.

treatment with H_2, was then treated with a pulse of CO (40 molecules of CO per Ir atom). The 2173-cm^{-1} band then disappeared as bands appeared at 2152 and 2130-cm^{-1}, along with a broad absorbance at 2077 cm^{-1} (Figure 6). On the basis of reported IR spectra of zeolite-supported iridium carbonyl species,[14] we assign the weak band at 2152 cm^{-1} to $Ir^{2+}(CO)$ species bonded to the amorphous regions of the support, and the band at 2130 cm^{-1} could be assigned to the aforementioned $Ir^{2+}(CO)_2$ species located in the crystalline region and/or to $Ir^{+}(CO)_2$ species located in the amorphous region of the support. The 2077-cm^{-1} band has been assigned on the basis of reported IR and EXAFS data to $Ir^{+}(CO)_3$ species,[9] and its broadness suggests the possible presence of $Ir^{0}(CO)$ species as well.[14] This sample was treated with ^{13}CO (Figure S7) to confirm the presence of the carbonyl ligand, with the results matching the expectation based on the calculated isotopic shift factor.[22] The EXAFS data do not resolve the matter, because the data were represented by two possible fits, with one or two carbonyl ligands bonded to the iridium (Table S6).

Oxidation states of iridium

As indicated by the IR data (Figure 1A) and the $Ir–Al_{zeolite}$ contribution in the EXAFS data (Table 1), all the iridium complexes in the zeolite are inferred to have been bonded at cation exchange positions, that is, near the Al sites. Alternatively, the IR spectra give evidence of the presence of iridium complexes bonded to the support not in these exchange positions but instead in the minor amorphous regions of the material, as suggested by the presence of the 2152- and 2130-cm^{-1} bands.

These inferences suggest the possibility of various oxidation states of iridium in the samples, and so the XANES data were examined to test the possibility. Data characterizing the sample initially incorporating $Ir(CO)_2$ complexes (Figure S10) remained essentially the same during the aforementioned treatments with H_2 (and with C_2H_4) at 298 K and 1 bar, results that indicate that a large fraction of the iridium remained in essentially the same oxidation state as it was at the beginning, Ir^{+}. Because the IR data suggest the presence of carbonyls of Ir^{2+} complexes, and because the XANES data do not give evidence of a change in the iridium oxidation state, we infer that the Ir^{2+} carbonyl complexes were only a small fraction of the total iridium, undetectable by XANES.

Instead, the XANES data give evidence of changes in the ligands bonded to the iridium. For example, the spectrum of the sample in which iridium was bonded to two CO ligands differs from that of the samples incorporating single CO ligands on iridium (Figure S10, inset).

Table 5. Calculated ligand dissociation energies (LDE) (in kcal/mol) for zeolite-supported Ir(CO)L at the B3LYP/aug-cc-pVDZ//$Al(OH)_4$ and B3LYP/CRENBL_ECP//Zeo-48T levels.

Ir(CO)L	$Al(OH)_4$		Zeo(48-T)	
	LDE(L)	LDE(CO)	LDE(L)	LDE(CO)
$Ir(CO)_2$	71.5	71.5	67.2	67.2
$Ir(CO)(C_2H_4)$	56.2	72.7	49.2	72.6
$Ir(CO)(C_2H_5)$	58.1	[a]	52.7	57.2[b],37.6[c]
Ir(CO)(H)	76.9	74.8	74.9	77.2
$Ir(CO)(H_2)$	51.7	74.8	47.6	76.1

[a] $Ir(C_2H_5)Al(OH)_4$ singlet relaxes into $Ir(C_2H_4)H$. Reaction energy for $Ir(CO)C_2H_5 \rightarrow Ir(C_2H_4)H + CO$ is calculated to be 51.3 kcal/mol. [b] Reaction energy for Zeo(48-T)-$Ir(CO)(C_2H_5)$ → Zeo(48-T)-$Ir(-H-C_2H_4)$ + CO. [c] Reaction energy for Zeo(48-T)-$Ir(CO)(C_2H_5)$ → Zeo(48-T)-$Ir(C_2H_4)(H)$ + CO.

Ligand dissociation energies

The experimental results show that the treatment in flowing H_2 does not directly remove the carbonyl ligands of the iridium dicarbonyl species under mild conditions (298 K and 1 bar). This observation is in accord with the predicted bond dissociation energies (Table 5), inasmuch as the Ir–H and Ir–CO ligand dissociation energies are comparable to each other, with the differences being within the accuracy of the calculations. The ligand dissociation energies calculated for the simple $Al(OH)_4$

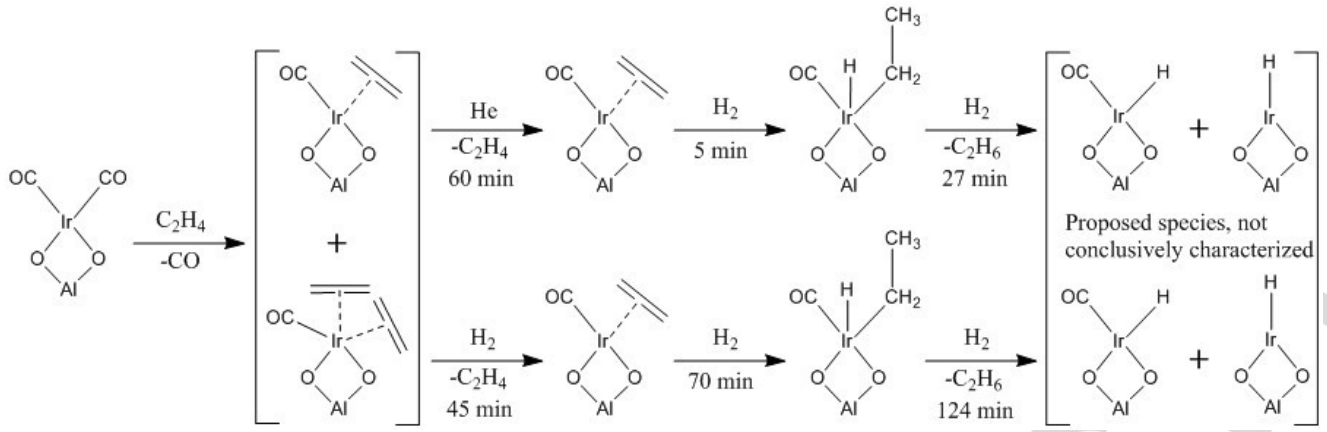

Scheme 1. Structural changes occurring in the iridium complexes bonded to the crystalline region of dealuminated HY zeolite initially present as $Ir(CO)_2$, when exposed to various gases at 298 K and 1 bar. The supported iridium complexes were identified on the basis of experimental results and DFT calculations. The suggested species at the right incorporating hydride ligands are less than fully characterized and regarded as tentative.

model and the much larger Zeo(48-T) model are in excellent agreement with each other and show that the ligand dissociation energies are dominated by the local site interactions about the metal center.

Discussion

The results presented here show that the ability of iridium in zeolite-supported iridium dicarbonyls to exchange a single carbonyl ligand with an alkene opens the opportunity to investigate the chemistry of a family of site isolated iridium carbonyl complexes incorporating alkene and hydride ligands. The remaining carbonyl ligand serves as an informative reporter ligand because of the sensitivity of the IR spectra in the carbonyl region to the neighboring ligands. Our results markedly expand previously reported data[9] characterizing the family of iridium complexes on the zeolite. Combining all the available data, we infer the reaction network shown in Scheme 1. We emphasize that the hydride-containing iridium carbonyl species are not conclusively characterized; comments about the identifications of the individual supported species are summarized in Table 6.

Elucidation of this reaction network was made possible by replacement of one of the carbonyl ligands on iridium with an alkene, which was then replaced by hydrogen. DFT calculations of zeolite-supported complexes for two models, an $Al(OH)_4$ model of the acid site and a larger model, Zeo(48-T),[26] show that the order of ligand dissociation energies for removal of the first ligand from iridium follows the trend CO > C_2H_4 > H_2 (Table 5), matching our experimental results. The Ir–CO bond has the highest dissociation energy, so that when the sample is treated with flowing ethylene, it is possible to remove only a single carbonyl ligand, followed by the replacement of the ethylene with hydrogen. The other carbonyl ligand remains bonded to the iridium throughout the treatments because neither ethylene nor hydrogen is able to remove the remaining strongly bonded carbonyl ligand.

We stress that this subtle chemistry of site-isolated iridium complexes requires a support that is a good electron-withdrawing ligand—when $Ir(CO)_2$ is bonded instead to the electron-donating MgO, it is not possible to replace any of the carbonyl ligands with C_2H_4 or H_2 under conditions of ambient temperature and pressure.[9] Thus, the zeolite is a valuable platform for the investigation of a family of nearly uniform site-isolated metal species, and these offer the opportunity to carry out catalysis experiments to determine the effects of various ligands on the catalytic performance.[8]

Conclusions

In summary, our results provide a reaction network characterizing a family of iridium carbonyl species supported on zeolite HY. Elucidation of the chemistry was facilitated by the strong bond between iridium and the carbonyl ligands, which made possible the selective replacement of one of the two carbonyl ligands initially bonded to the iridium with more weakly bonded ligands such as ethylene. Moreover, by taking advantage of the high degree of uniformity of the supported iridium complexes, it was possible to follow the replacement of the ethylene with hydrogen, because ethyl was observed as an intermediate as evidenced by mass spectrometry together with IR, EXAFS and DFT calculations. The DFT calculations are consistent with the experimental spectra, providing support for the identification of the species involved; some of the supported species could not have been identified without the calculations, and the evidence of the exact nature of the iridium deuteride species is less than conclusive. The results show that the ligand dissociation energies are dominated by local site interactions about the metal center.

Table 6. Summary of zeolite-supported iridium carbonyl complexes formed from treatments of supported $Ir(CO)_2$ complexes in H_2 and C_2H_4 at 298 K and 1 bar.

Iridium-containing species in sample	Treatment/ conversion	*ν*(C–O) cm^{-1}	*ν*(Ir–H) cm^{-1}	*ν*(Ir–D) cm^{-1}	Comments
$Ir(CO)_2$	In helium	2109 and 2038	[a]	[a]	$CO/^{13}CO$ isotopic exchange confirms the presence of the carbonyl ligands. EXAFS data confirm the presence of two CO ligands bonded to each Ir atom. DFT calculations of the C–O stretching vibration with the $Al(OH)_4$ and the Zeo(48-T) model bracket the experimental ν_{CO} values with good agreement.
$Ir(CO)(C_2H_4)_2$	Formed from $Ir(CO)_2$ in flowing C_2H_4	2087	[a]	[a]	$CO/^{13}CO$ isotopic exchange confirms the presence of carbonyl ligands. EXAFS data confirm the presence of a mixture of species containing one CO and one or two ethylene ligands bonded to each Ir atom. Assignment is consistent with previous work.[9] DFT calculations of the C–O stretching vibration with the $Al(OH)_4$ and the Zeo(48-T) model bracket the experimental values with good agreement.
$Ir(CO)(C_2H_4)$	Formed from $Ir(CO)_2$ after flow of C_2H_4 followed by helium	2055	[a]	[a]	
$Ir(CO)(C_2H_5)$	Formed from preceding sample in flowing H_2. See Scheme 1 for details.	2075	[b]	[a]	$CO/^{13}CO$ isotopic exchange confirms the presence of carbonyl ligands. EXAFS data confirm the presence of one ethyl and one CO bonded to each Ir atom. DFT calculations of the C–O stretching vibration with the $Al(OH)_4$ and the Zeo(48-T) model bracket the experimental values with good agreement.
Ir(CO)(H)	Formed from preceding sample in flowing H_2. See Scheme 1 for further details.	2068	[b]	1509	$CO/^{13}CO$ isotopic exchange confirms the presence of carbonyl ligands. EXAFS data confirm the presence of one CO bonded to each Ir atom. DFT calculations of the C–O stretching vibration with the $Al(OH)_4$ and the Zeo(48-T) model bracket the experimental values with good agreement. HD isotopic exchange with D_2O followed by H_2 confirms the presence of deuteride/hydride species. DFT calculations of the Ir–D stretching vibration with the $Al(OH)_4$ and the Zeo(48-T) model give slightly greater values (1591/1674 cm^{-1}, respectively) than the experimental value of 1509 cm^{-1}.
$Ir(CO)(C_2H_4)(H)$		[b]	[b]		$CO/^{13}CO$ isotopic exchange confirms the presence of carbonyl ligands. EXAFS data suggest the presence of CO and ethylene or ethyl based on models with physically realistic values; however, these models are characterized by less than satisfactory fits of individual shells, and consequently they were discarded. DFT calculations of the Ir–D stretching vibration of $Ir(D)(C_2H_4)$ and $Ir(D)(C_2D_4)$ species are in good agreement with the experimental value. H–D isotopic exchange with D_2O followed by H_2 confirms the presence of deuteride/hydride species.
$Ir(CO)(C_2H_5)(H)$		[b]	[b]		
Ir(H)		[a]	[b]		HD isotopic exchange with D_2O followed by H_2 confirms the presence of deuteride species. DFT calculations of the Ir–D stretching vibration with the $Al(OH)_4$ and the Zeo(48-T) model give slightly larger values (1578/1657 cm^{-1}, respectively) than the experimental value of 1509 cm^{-1}. NOTE: The absence of IR bands in the Ir–H region along with the inconclusive assignment of the deuteride species characterized by the 1509-cm^{-1} band neither confirms nor denies the existence of this complex.

[a] Not applicable. [b] Not observed.

Experimental and Computational Section

$Ir(CO)_2$/HY zeolite synthesis: The support, dealuminated zeolite HY (Zeolyst International, CBV760, Si/Al atomic ratio ≈ 30, according to the manufacturer), was calcined in O_2 (Praxair, 99.5%) at 773 K for 2 h, followed by evacuation at 773 K for 14 h. After calcination, the support was stored in an argon-filled glovebox. The precursor $(Ir(CO)_2(acac)$, 99%, Strem) (acac is acetylacetonate, $C_5H_7O_2^-$) and the calcined zeolite were combined into a slurry with dried, deoxygenated *n*-pentane (Fisher,

99%) and stirred for 24 h. The solvent was then removed by evacuation for a day. The resultant powder, containing 1 wt% iridium, was stored in the glovebox. H_2 was supplied by Airgas (99.999%) and purified by passage through traps containing reduced Cu/Al_2O_3 and activated zeolite 4A to remove traces of O_2 and moisture, respectively. Helium (Airgas, 99.999%) and ethylene (Airgas, 99.5%) were purified by passage through similar traps. CO (10 mol%) in helium was purified by passage through a trap containing particles of activated γ-Al_2O_3 and of zeolite 4A to remove any traces of metal carbonyls from the high-pressure gas cylinders and moisture, respectively. D_2O (99.9%) and ^{13}CO (99%) were purchased from Cambridge Isotope Laboratories.

IR Spectroscopy: IR spectra of the solid samples were recorded with a Bruker IFS 66v/S spectrometer; the spectral resolution was 2 cm^{-1}. Each sample (~30 mg) was pressed into a thin wafer and loaded between two KBr windows in a cell in the argon-filled glovebox. The cell was sealed, transferred, and connected to a flow system that allowed recording of spectra while flowing gases passed through and around the sample. The spectra were recorded at 298 K with exclusion of air and moisture. Each reported spectrum is the average of 64 scans.

Mass Spectrometry: Mass spectra of the effluent gases from the flow system, some produced by reaction with the sample, were measured with an online Balzers OmniStar mass spectrometer running in multi-ion monitoring mode. These data were collected as IR spectra were being recorded. Changes in the signal intensities of ethane (*m*/*z* = 30, 28, 27, 26), ethylene (*m*/*z* = 28, 27, 26), and H_2 (*m*/*z* = 2) were recorded.

X-ray Absorption Spectroscopy: The X-ray absorption spectra were recorded at X-ray beamline 10-ID-B (MR-CAT) at the Advanced Photon Source (APS) at Argonne National Laboratory. The storage ring electron energy and ring current were 7 GeV and 105 mA, respectively, and the monochromator was a double-crystal Si(111). The monochromator was detuned by 20% at the Ir L_{III} edge to minimize the effects of higher harmonics in the X-ray beam. Each powder sample was loaded into a cell that served as a flow reactor,[27] which was sealed inside an argon-filled glove box. Spectra were collected in transmission mode with the sample in the presence of flowing gases at 298 K and 1 bar. XANES and EXAFS spectra were recorded simultaneously at intervals of 4 min.

Computational Methods: Two models of the zeolite were used for the calculations. A simple model of the zeolite surface site, represented as ML_n–$Al(OH)_4$, (where M is Ir and L represents the ligands), was chosen because earlier work showed that it provides good agreement with the structural and vibrational frequency measurements determined by experiment for analogous rhodium complexes,[28] as well as for N_2 complexes when compared with experiment and with larger models of the acidic zeolite site.[26] Geometry optimization and second-derivative frequency calculations of the supported iridium complexes for this model were carried out by using DFT with the B3LYP exchange-correlation functional,[29,30] the aug-cc-pVDZ basis set[31] on H, C, N, O, and Al, and the aug-cc-pVDZ-pp basis set and pseudopotential[31] on iridium. The electronic structure method for the small model is the same as that used before for the aforementioned rhodium complexes, which consistently showed good agreement between calculated and experimental values.[28] We also performed calculations with a larger zeolite model (Zeo(48-T) where T is the number of Si + Al atoms. The calculations of the Zeo(48-T) structure were done with the same B3LYP functional and the CRENBL basis sets and effective core potentials for all atoms[32-33] except for H.[34] The basis sets are of double-ζ quality due to the size of the system. All of the calculations were done by using the Gaussian 03/09 program suites.[32] Calculations for several more complex models of comparable supported iridium species have also been reported,[26] confirming the appropriateness of the choice of the simplified model for the comparisons with experiment reported here. The Zeo(48-T) model is a relatively realistic model obtained by truncating the zeolite crystal structure, and it was used to test the small $Al(OH)_4$ model. The Zeo(48-T) model can represent the actual zeolite super-cage, especially for properties such as the rigidness of the zeolite framework, the local flexibility of the -Si-O-Si- interactions in the backbone, etc., which can significantly affect the local environment of the iridium complexes. The geometry optimization calculations based on the larger Zeo(48-T) model shows that Ir(I) complexes with more than one ligand do not form bonds with the neighbouring surface sites whereas most of the mono-ligand and the naked Ir(I) complexes form a bond with a third oxygen atom from the neighbouring surface sites. (The exception is $Ir(C_2H_4)$, which slightly prefers to bind to 2 O atoms rather than 3 O atoms.) All calculations were done with the Gaussian09 code[35] on computers in the Dixon laboratory or the Alabama Supercomputing Center.

Acknowledgements

This work was supported by the U.S. Department of Energy (DOE), Office of Science, Basic Energy Sciences (BES), Grants DE-FG02-04ER15513 (C.M.M.) at the University of California, Davis, and DE-SC0005822 (M.C.) at The University of Alabama. C.M.M. was supported in part by the UC-MEXUS-CONACYT doctoral fellowship program. M.C. was also sponsored by the DOE Office of Advanced Scientific Computing Research and performed calculations at the Oak Ridge National Laboratory, which is managed by UT-Battelle, LLC, under Contract No. De-AC05–00OR22725. D.A.D. thanks the Robert Ramsay Chair Fund of The University of Alabama for support. This research was aided by resources of the Advanced Photon Source, a DOE Office of Science User Facility operated for the DOE Office of Science by Argonne National Laboratory (ANL) under Contract No. DE-AC02-06CH11357. Experiments were performed at beamline 10-ID-B (the MRCAT) at ANL; MRCAT operations are supported by the DOE and the MRCAT member institutions. We thank HPCAT (Sector 16) of APS for access to a glovebox for sample preparation and storage during our beam time. HPCAT operations are supported by DOE-NNSA under Award No. DE-NA0001974 and DOE-BES under Award No. DE-FG02-99ER45775, with partial instrumentation funding by NSF. APS is supported by DOE-BES under Contract No. DE-AC02-06CH11357

Keywords: zeolite • supported iridium complexes • DFT calculations • CO probe molecule • iridium carbonyls • iridium hydride

[1] M. Beller, X.-F. Wu in *Transition Metal Catalyzed Carbonylation Reactions: Carbonylative Activation of C-X Bonds*, Springer-Verlag Berlin Heidelberg **2013**, p. 18.

[2] Y. V. Kissin in *Alkene Polymerization Reactions with Transition Metal catalysts*, Vol. 173 Elsevier B. V., **2008**, p. 3.

[3] D. Yardimci, P. Serna, B. C. Gates, *ChemCatChem* **2012**, *4*, 1547–1550.

[4] I. Ogino, B. C. Gates, *J. Am. Chem. Soc.* **2008**, *130*, 13338–13346.

[5] A. J. Liang, V. A. Bhirud, J. O. Ehresmann, P. W. Kletnieks, J. F. Haw, B. C. Gates, *J. Phys. Chem. B* **2005**, *109*, 24236–24243.

[6] A. Uzun, V. A. Bhirud, P. W. Kletnieks, J. F. Haw, B. C. Gates, *J. Phys. Chem. C* **2007**, *111*, 15064–15073.

[7] J. C. Fierro-Gonzalez, B. G. Anderson, K. Ramesh, C. P. Vinod, J. W. Niemantsverdriet, B. C. Gates, *Catal. Lett.* **2005**, *101*, 265–274.

[8] P. Serna, B. C. Gates, *Acc. Chem. Res.* **2014**, *47*, 2612–2014.

[9] J. Lu, P. Serna, B. C. Gates, *ACS Catal.* **2011**, *1*, 1549–1561.

[10] J. Dwyer, P. J. O'Malley, in *Keynotes in Energy-Related Catalysis*, Vol. 35, (Ed. S. Kaliaguine) Elsevier: Amsterdam, **1988**, p. 28.

[11] O. Cairon, T. Chevreau, J. C. Lavalley, *J. Chem. Soc., Faraday Trans.* **1998**, *94*, 3039–3047.

[12] A. Uzun, V. A. Bhirud, P. W. Kletnieks, J. F. Haw, B. C. Gates *J. Phys. Chem. C* **2007**, *111*, 15064–15073.

[13] F. Solymosi, E. Novák, A. Molnár *J. Phys. Chem.* **1990**, *94*, 7250–7255.

[14] M. Mihaylov, E. Ivanova, F. Thibault-Starzyk, M. Daturi, L. Dimitrov, K. I. Hadjiivanov *J. Phys. Chem. B* **2006**, *110*, 10383–10389.

[15] H. Miessner, I. Burkhardt, D. Gutschick, A. Zecchina, C. Morterra, G. Spoto, *J. Chem. Soc. Faraday Trans. 1* **1989**, *85*, 2113–2126.

[16] I. Ogino, B. C. Gates *J. Phys. Chem. C* **2010**, *114*, 2685–2693.

[17] J. Lu, P. Serna, C. Aydin, N. D. Browning, B. C. Gates *J. Am. Chem. Soc.* **2011**, *133*, 16186–16195.

[18] J. Lu, C. Aydin, N. D. Browning, B. C. Gates *Langmuir* **2012**, *28*, 12806–12815.

[19] C. Martinez-Macias, P. Xu, S.-J. Hwang, J. Lu, C.-Y. Chen, N. D. Browning, B. C. Gates, *ACS Catal.* **2014**, *4*, 2662–2666.

[20] K. P. Huber, G. Herzberg in *Molecular Spectra and Molecular Structure iV. Constants of Diatomic Molecules*, Van Nostrand Reinhold: New York, **1979**.

[21] W. C. Conner, G. M. Pajonk, S. J. Teichner *Adv. Catal.* **1986**, *34*, 1–79.

[22] K. I. Hadjiivanov, G. N. Vayssilov *Adv. Catal.* **2002**, *47*, 307–511.

[23] Criss, R. E. in *Principles of Stable Isotope Distribution*, Oxford University Press Inc. **1999**, p. 60.

[24] R. H. Crabtree in *The Organometallic Chemistry of the Transition Metals*, Wiley, **2009**, p. 285.

[25] J. Lu, C. Aydin, N. D. Browning, B. C. Gates, *J. Am. Chem. Soc.* **2012**, *134*, 5022–5025.

[26] D. Yang, M. Chen, C. Martinez-Macias, D. A. Dixon, B. C. Gates *Chem. Eur. J.* **2015**, *21*, 631-640.

[27] J. F. Odzak, A. M. Argo, F. S. Lai, B. C. Gates, *Rev. Sci. Instrum.* **2001**, *72*, 3943–3945.

[28] A. J. Liang, R. Craciun, M. Chen, T. G. Kelly, P. W. Kletnieks, J. F. Haw, D. A. Dixon, B. C. Gates, *J. Am. Chem. Soc.* **2009**, *131*, 8460–8473.

[29] (a) C. Lee, W. Yang, R. G. Parr *Phys. Rev. B*, **1988**, *37*, 785–789. (b) B. Miehlich, A. Savin, H. Stoll, H. Preuss *Chem. Phys. Lett.* **1989**, *157*, 200–206.

[30] A. D. Becke *J. Chem. Phys.* **1993**, *98*, 5648–5652.

[31] R. A. Kendall, T. H. Dunning, R. J. Jr. Harrison, *Chem. Phys.* **1992**, *96*, 6796–6806.

[32] L. F. Pacios, P. A. Christiansen, *J. Chem. Phys.* **1985**, *82*, 2664–2671.

[33] R. B. Ross, J. M. Powers, T. Atashroo, W. C. Ermler, L. A. Lajohn, P. A. Christiansen, *J. Chem. Phys.* **1990**, *93*, 6654-6670.

[34] T. H. Dunning Jr., P. J. Hay, in *Methods of Electronic Structure Theory, Modern Theoretical Chemistry, Vol. 3* (Ed.: H. F. Schaeffer), III, Plenum Press, New York,, **1975**, 1-27.

[35] Gaussian 09, M. J. Frisch, et al. Wallingford CT, **2009**. The full reference is available in the Supporting Information.

Entry for the Table of Contents

FULL PAPER

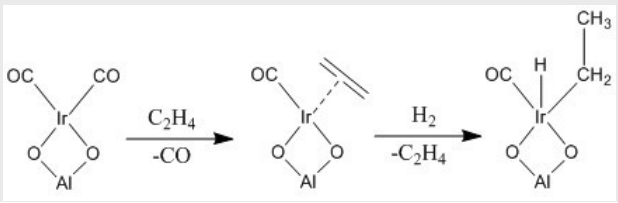

A family of HY zeolite-supported organoiridium carbonyl complexes was formed by reaction of $Ir(CO)_2(acac)$ (acac = acetylacetonate) to form supported $Ir(CO)_2$ complexes, which were treated with flowing gas-phase reactants at 298 K and 1 bar. The crystalline support, with its nearly uniform array of bonding sites for the supported iridium species, allowed precise structure determinations, with the experimental results in good agreement with DFT calculations.

*Claudia Martinez-Macias, Mingyang Chen, David A. Dixon, and Bruce C. Gates**

Page No. – Page No.

Single-Site Zeolite-Anchored Organoiridium Carbonyl Complexes: Characterization of Structure and Reactivity by Spectroscopy and Computational Chemistry